JOURNAL OF MATERIALS SCIENCE 22 (1987) 1769–1772

Kinetics of intermetallic compound growth between nickel, electroless Ni–P, electroless Ni–B and tin at 453 to 493 K

W. J. TOMLINSON, H. G. RHODES
Department of Materials, Coventry Polytechnic, Coventry CV1 5FB, UK

The growth kinetics, crystal structure, and morphology of the intermetallic compounds formed between nickel, electroless Ni–P and electroless Ni–B coatings with tin at 453 to 493 K for times up to 506 h have been determined by microscopical and X-ray diffraction techniques. The compound Ni_3Sn_4 was formed. All kinetics followed as parabolic law with activation energies of 128.0, 130.4, and 122.3 kJ mol^{-1} for the Ni/Sn, Ni–P/Sn and Ni–B/Sn systems, respectively. The rate of growth of Ni_3Sn_4 in the Ni/Sn and Ni–P/Sn systems were similar but the rate of growth in the Ni–B/Sn system was five times faster. Pores occurred in the intermetallic compound formed in the Ni–P/Sn system and these are discussed in relation to the density of the phases.

1. Introduction

Intermetallic compounds frequently form and grow at the interface of two metals by reaction diffusion. In some cases the compounds have useful properties and are made by controlled heat-treatments, for example, the formation of Nb_3Sn in the Nb–Sn system [1]. However, the crystal structures are usually complex [2], and the compounds are characteristically brittle and typically have poor wettability [2–4]. Both these properties are particularly undesirable in soldered joints where the presence of intermetallic compounds may impair solderability [3–6], or lead to mechanical failure by fracture or to the degradation of the electrical properties of the conductor and connections [7, 8]. Tin is the basis of many solders and tin and tin–lead coatings are also frequently used to promote and maintain (by minimizing atmospheric corrosion) solderability of components stored before use [9]. Intermetallic compounds may grow readily at room temperature [10, 11], and their formation during shelf storage reduces solderability, increases the risk of cracking, and reduces the amount of tin left to form the solder joint [6, 9]. An associated problem with substrates containing zinc is the selective corrosion of zinc during storage and service to form surface reaction products, and these products also reduce solderability and joint performance and reliability in service [9].

To minimize both interdiffusion to form intermetallic compounds and diffusion of zinc to form reaction products, a readily solderable undercoat of copper, cobalt, or nickel may be used to produce a diffusion barrier [3, 9], and the use of nickel has become accepted commercial practice [12]. Nickel reacts with tin at room temperature to form Ni_3Sn_4 [10, 11]. With electroplated nickel the compound has the empirical formula Ni_3Sn_8 and a lath-like structure which rapidly penetrates the tin coating and reduces the solderability [4]. At higher temperatures (up to 170° C) a continuous layer of Ni_3Sn_4 forms at the nickel interface and a smaller amount of a discontinuous acicular phase also forms [8]. The crystal structure, amount, and morphology of the intermetallic compounds that form depend on the kind of metal (whether bulk, electrolytic, which electrolytic process, surface preparation, etc.) and the temperature and time of diffusion.

Electroless nickel is an alloy containing nominally either 5 to 10% P or about 0.5% B. It is used increasingly in place of conventional electrolytic coatings, particularly with respect to the uniformity of the deposit and the ability to plate on non-metallic substrates [13, 14]. The properties of both types of electroless nickel coatings may be quite different from those of electrolytic nickel and nickel [13, 14]. No information is available on the reaction of electroless nickel with tin or tin-based solders and the present work investigates the reaction of electroless Ni–P and electroless Ni–B with tin in the temperature range 453 to 493 K. For comparison, the behaviour of a commercial nickel is also examined.

2. Experimental procedure

Commercial nickel sheet and electroless nickel coatings were used. The nominal compositions were: Ni200 of composition (wt %) C 0.15, Mn 0.35, Fe 0.4, S 0.01, Si 0.35, Cu 0.25, and B and P each less than 40 p.p.m., electroless nickel phosphorus (ENP) of composition 10% P, and electroless nickel boron (ENB) of composition 0.25% B. The Ni200 was in the form of annealed sheet and the electroless nickel was as a coating on a mild steel substrate. Typically the coatings were 20 μm thick, but in some cases the coatings were about 10 μm thick. All samples were plated together with 20 μm of bright pure tin (about 99.9%) from an acid sulphate bath. The coatings were applied

0022–2461/87 $03.00 + .12

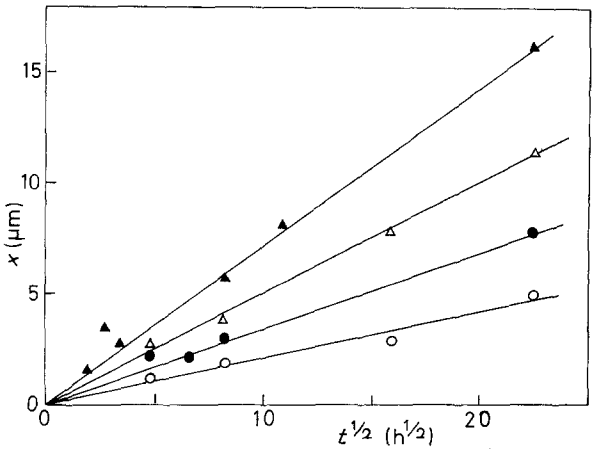

Figure 1 Intermetallic thickness, x, as a parabolic function of time t, in the Ni/Sn system at (▲) 493 K, (△) 483 K, (●) 473 K and (○) 453 K.

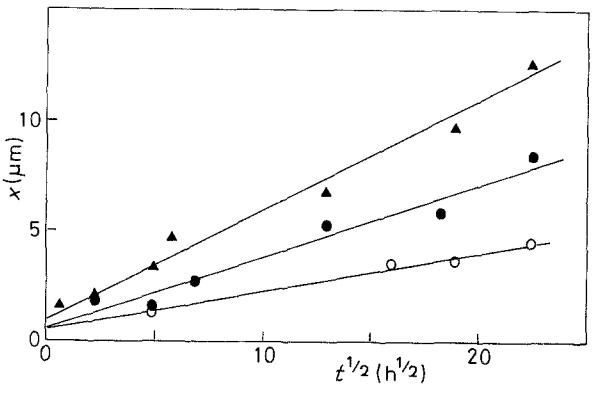

Figure 2 Intermetallic thickness, x, as a parabolic function of time, t, in the ENP/Sn system at (▲) 493 K, (●) 473 K and (○) 453 K.

commercially by Montgomery Plating (tin and ENP) and Shipley Chemicals (ENB). After plating, specimens 10 mm × 10 mm were cut using a rotary saw. Diffusion anneals were in an air-circulating oven. The maximum temperature variation at 220° C over 10 days was less than 1 K.

Heat-treated specimens were mounted in cold-setting resin and polished on SiC papers. A final polish on a hard 2 to 6 μm diamond cloth was found to give the sharpest edge preparation. The intermetallic layer was examined on a calibrated projection microscope at a magnification of 1500, and 15 random measurements of the thickness taken. Conventional scanning electron mciroscopy (SEM), EDAX microanalysis and X-ray diffraction (diffractometer and Läue back-scatter) were used to examine the compounds. In some cases, the overlying tin layer was chemically stripped [6]. A simple assessment of solderability was also made by measuring the area of spread of 180 mg of 60 Sn–40 Pb solder on the fluxed (proprietry resin base) surface of nickel at 250° C for 30 min.

3. Results

A single-phase layer was formed in each system. The layers were relatively uniform in thickness with the coefficient of variation of the 15 measurements on each specimen ranging from 2.6 to 15.7, 4.5 to 19.6, and 7.4 to 35.7 for the Ni/Sn, ENB/Sn, and ENP/Sn systems, respectively. In each case the high values correspond to the low temperature and small time exposure conditions. Scanning electron microscopy was used to check the accuracy of the optical measurements and the results presented in Table I show an excellent agreement. The mean thickness of the layers are shown in parabolic form in Figs 1 to 3. It is seen that the layer thickness in the Ni/Sn system (Fig. 1) extrapolates to a zero intercept whereas in the EN/Sn systems (Figs 2 and 3) the layer thickness extrapolates to about 1 μm at zero time. This is probably due to a slight roughness of the EN coatings compared with the polished nickel sheet which will give a faster reaction rate. The parabolic kinetic law is followed reasonably well (Figs 1 to 3), and the associated Arrhenius functions and parameters are given in Fig. 4 and Table II, respectively. The activation energies are similar for all systems but the growth rate of the intermetallic layer is five times faster in the ENB/Sn system.

Typical metallographic structures are shown in Figs 5 to 7. It was found that the sharpest intermetallic compound/tin interface suitable for optical measurements was with a partial diamond polish leaving residual scratches normal to the layer. This kind of preparation is shown in Fig. 5 which also illustrates the uniform thickness and density of the intermetallic compound which forms on the electroless nickel boron coating. Fig. 6 shows a typical SEM photograph used to examine and measure some of the thinnest intermetallic compounds. The intermetallic compound formed in the Ni/Sn system was similar to that formed in the ENB/Sn system (Figs 5 and 6), and in both cases the layer was unform in thickness and free from pores. In contrast, the layer formed on the electroless nickel phosphorus substrate (Fig. 7) consisted of chunky grains 1 to 2 μm diameter with an occasional intergrain pore (indicated by a circle in Fig. 7), and an irregular interface with the tin. However, it is clear that the irregular compound/tin interface in the ENP/Sn systems (Fig. 7) did not invalidate the parabolic kinetic law (Fig. 2). A dark etching zone occurs in the electroless nickel phosphorus about 7 μm thick (Fig. 7). This is caused by an accumulation of phosphorus and is discussed later. Scanning electron microscopy of heavily etched cross sections and chemically stripped surfaces of the intermetallic compounds confirmed that the microstructure of the compound formed in the Ni/Sn and ENB/Sn systems were fine-grained and

TABLE I Comparison of the thickness of the intermetallic compound formed at 493 K after 506 h measured optically and using the scanning electron microscope

System	Thickness (μm)	
	Optical	SEM
Ni200/Sn	16.2	16.0
ENP/Sn	12.7	12.3
ENB/Sn	35.6	36.0

TABLE II Arrhenius parameters for parabolic growth

	Ni/Sn	ENP/Sn	ENB/Sn
Activation energy, E(kJ mol^{-1})	128.0	130.4	122.3
k_0(10^{-3} m^2 sec^{-1})	3.22	4.23	3.02

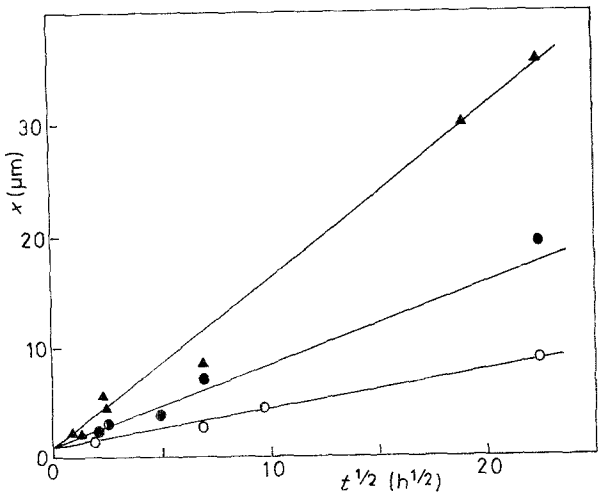

Figure 3 Intermetallic thickness, x, as a parabolic function of time t, in the ENB/Sn system at (▲) 493 K, (●) 473 K and (○) 453 K.

dense, whereas the microstructure of the compound formed in the ENP/Sn system consisted of coarse grains and contained some intergrain pores.

EDAX line analyses across the intermetallic layers showed a single continuous and uniform composition of nickel and tin in all three systems with the measured atomic ratio of nickel to tin approximately 0.8. This is close to the formula Ni_3Sn_4. Phosphorus could not be detected in the intermetallic layer formed on the ENP and there was a corresponding accumulation of phosphorus in the EN. Some of the phosphorus which was rejected into the electroless nickel during growth of the layer precipitated and could be seen as an etching region about 7 μm thick (Fig. 7).

There was an excellent correlation between the X-ray diffraction d-spacings from the intermetallic layers of all three systems and those of the compound Ni_3Sn_4 in the ASTM card index [15]. However, peak broadening occurred and the prominant peak corresponding to a d-spacing of 0.206 nm was absent. Peak broadening occurs with Ni_3Sn_4 [16] and is thought to be due to the presence of two tin environments in Ni_3Sn_4 both of which are distorted [16, 17]. In the

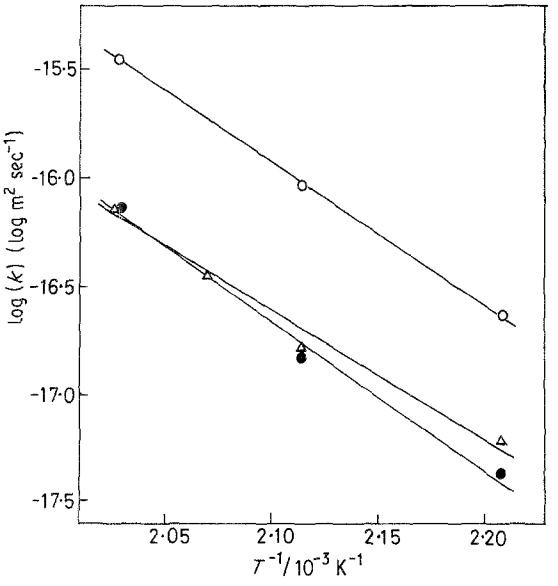

Figure 4 Arrhenius function of the parabolic kinetic law $x^2 = 2kt$. (○) ENB/Sn, (△) Ni/Sn, (●) ENP/Sn.

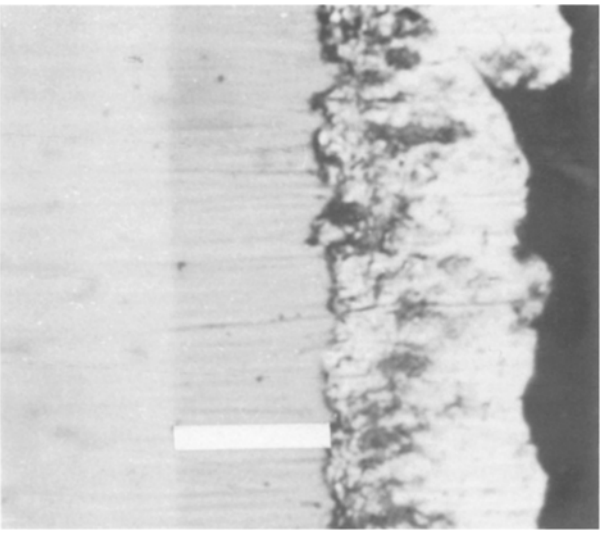

Figure 5 Intermetallic compound formed in the Ni–B/Sn system after 34 h at 493 K. Compound thickness identified with the marker (12.7 μm). Tin on the right.

present work it is considered that the 0.206 nm peak is absent because it has merged with the neighbouring prominant and broad 0.203 nm peak. A back scattered Läue photograph of the layer formed on the nickel did not indicate any preferred orientation of the Ni_3Sn_4 compound.

4. Discussion

The intermetallic compound Ni_3Sn_4 is the only phase formed in all the systems over the whole range of exposure conditions and, except for an initial rapid reaction in the electroless nickel systems, it forms according to the parabolic kinetic law $x^2 = 2kt$ (Figs 1 to 3). Ni_3Sn_4 has only a narrow range of homogeneity [18] and in such cases the intermetallic growth occurs according to the parabolic growth law with the parabolic (practical) reaction rate constant given by [19]

$$\bar{k} = (\bar{D}_{Ni}/3 + \bar{D}_{Sn}/4)(\Delta G^{\ominus}/RT)$$

The bars indicate average value and $\Delta G^{\ominus}$ is the Gibbs function for the reaction $3\,Ni + 4\,Sn = Ni_3Sn_4$.

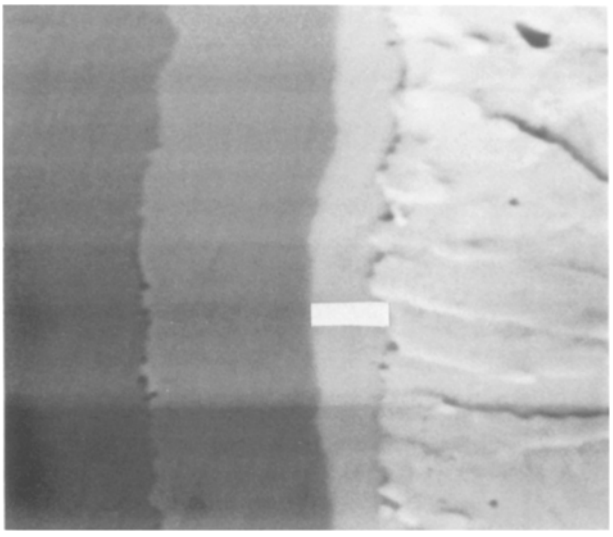

Figure 6 Intermetallic compound formed in the Ni–B/Sn system after 95 h at 453 K. Compound thickness identified with the marker (1.5 μm). Tin on the right.

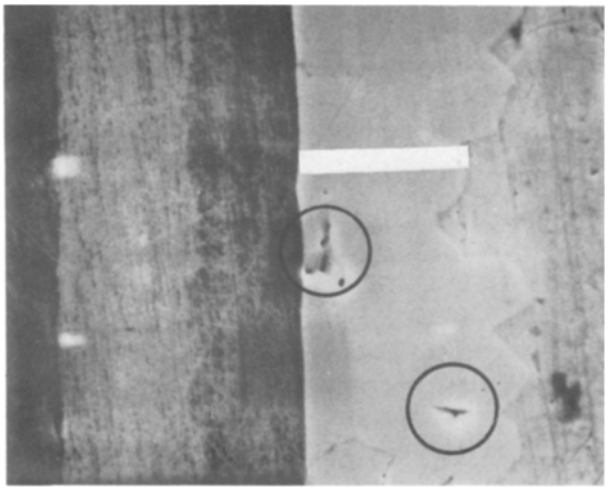

Figure 7 Intermetallic compound formed in the Ni–P/Sn system after 506 h at 493 K. Compound thickness identified with the marker (10 μm). Tin on the right. Intergrain pores in the compound identified by circles. Note the precipitation due to phosphorus accumulation in the Ni–P.

Thermodynamic data for the reaction and for the component diffusion coefficients are not available and so the model may not be confirmed. However, it is clear from the similar activation energies (Table II) that the same mechanism of diffusion is occurring in Ni_3Sn_4 in each system. The defect concentrations influence the diffusion rates [19], and the similar values of the activation energies and rate constants for the formation of Ni_3Sn_4 in the Ni/Sn and ENP/Sn systems (Fig. 4) indicates a similar defect structure and concentration. This is supported by the absence of phosphorus from the Ni_3Sn_4 layer in the ENP/Sn system and hence the absence of any possible extrinsic defects. The increased reaction rate in the ENB/Sn system along with the same activation energies implies an increase in the defect concentration of Ni_3Sn_4. Unfortunately, boron could not be monitored using the present EDAX system and its presence and possible effects could not be determined. However, from the present results we must assume some solubility of boron in the Ni_3Sn_4 and the generation of extrinsic defects.

The morphology of the Ni_3Sn_4 in the ENP/Sn has two features that do not occur in the other systems. Intergranular voids are occasionally present in the Ni_3Sn_4 and the Ni_3Sn_4/Sn interface has a course irregular structure (Fig. 7). The densities of tin, Ni_3Sn_4, and nickel are 7.30, 8.42, and 8.90 $Mg\,m^{-3}$, respectively [10], and the densities of ENB and ENP are 8.90 and 8.1 $Mg\,m^{-3}$, respectively [20]. Hence the following inequalities exist:

$$\varrho(\mathrm{Sn}) < \varrho(\mathrm{Ni_3Sn_4}) < \varrho(\mathrm{Ni\ or\ ENB})$$

$$\varrho(\mathrm{Sn}) < \varrho(\mathrm{Ni_3Sn_4}) > \varrho(\mathrm{ENP})$$

When either the tin or ENP is replaced by Ni_3Sn_4 of higher density (lower specific volume) the Ni_3Sn_4 will be in tension. It seems that voids that form in the ENP/Sn system (Fig. 7) do so to relieve the tension and to accommodate the density increase. In contrast, in the Ni/Sn and ENB/Sn systems, the effects of the density change of Ni_3Sn_4 are to some extent offset by the density changes of the tin and the nickel, and so the Ni_3Sn_4 layer is relatively compact. The cause of the irregular Ni_3Sn_4/Sn interface in the ENP/Sn system is unclear, but it may also be associated with tension and voiding in the Ni_3Sn_4 layer.

Finally, we comment on the solderability of the electroless nickel coatings. The area of spread of 180 mg of solder on the nickel, ENP, and ENB surface was 38, 43, and 58 mm^2, respectively, and it is seen on the basis of this simple test that the ENB has the best solderability. In terms of the use as a barrier layer it is unfortunate that the ENB also has the highest reaction rate with tin. It must also be remembered, however, that the present results may not extrapolate to long-term room-temperature behaviour, although it is possible that the lath-like structures which rapidly form on electrolytic nickel and rapidly penetrate the tin coating and reduce solderability [4] may not, with great advantage, form with the electroless nickel coatings.

Acknowledgements

The authors wish to thank H. Wiggin for the supply of Ni200, Shipley Chemicals for the supply of electroless nickel boron, Montgomery Plating for the supply of electroless nickel phosphorus and electrolytic tin, and Dr R. Carey and C. Dawson for the SEM/EDAX results.

References

1. S. K. AGARWAL, S. B. SAMANTA, V. K. BATRA and A. V. NARLIKAR, *J. Mater. Sci.* **19** (1984) 2057.
2. F. LAVES, in "Intermetallic compounds", edited by J. H. Westbrook (Wiley, New York, 1967) pp. 129–143.
3. R. J. KLEIN WASSINK, "Soldering in Electronics", (Electrochemical Publications, Ayr, 1984) pp. 98–101.
4. A. C. HARMAN, "Proceedings of Internepcon, Brighton, 1978, Edited by H. G. Mansfield (Kilver Communications S.A, Surbitan, UK 1978) pp. 42–9.
5. P. E. DAVIS, M. E. WARWICK and P. J. KAY, *Plating Surf. Fin.* **69** (1982) 72.
6. P. E. DAVIS, M. E. WARWICK and S. J. MUCKETT, *ibid.* **70** (1983) 49.
7. K. N. TU, *Acta Metall.* **21** (1973) 347.
8. P. J. KAY and C. A. MACKAY, *Trans. I. Met. Fin.* **54** (1976) 68.
9. *Idem, ibid.* **57** (1979) 169.
10. K. N. TU and R. ROSENBERG, *Jap J. Appl. Phys.* **Suppl. 2** (1) (1974) 633.
11. Z. MARINKOVIC and V. SIMIC, *Thin Solid Films* **98** (1982) 95.
12. British Standards 1872, 1964.
13. S. S. TULSI, *Trans. Inst. Metal Finish.* **61** (1983) 147.
14. D. W. BAUDRAND, *Plating Surface Finish.* **70** (1983) 24.
15. X-ray Powder Diffraction File, ASTM STP 48 (American Society for Testing and Materials, Philadelphia, 1982).
16. D. NIAL, *Svensk. Kem. Tid.* **59** (1983) 165.
17. J. SILVER, C. A. MACKAY and J. D. DONALDSON, *J. Mater. Sci.* **11** (1976) 836.
18. Metals Handbook, 8th edn, Vol. 8 (1973) (American Society of Metals, Ohio, 1973) p. 325.
19. H. SCHMALZRIED, (Tranlated by A. D. Pelton), "Solid State Reactions" (Academic Press, New York, 1974).
20. "Niposit 65 and Niposit 468 Electroless Nickel" (Shipley Chemicals, Humber Avenue, Coventry, UK) February 1980.

Received 25 June
and accepted 9 September 1986